INCLUSIVE SINGLE-PARTICLE DISTRIBUTIONS IN $\bar{p}p$ INTERACTIONS AT 14.75 GeV/c

F.T. Dao, J. Lach and J. Whitmore
Fermi National Accelerator Laboratory, Batavia, Illinois 60510, U.S.A.

(Presented by F.T. Dao and J. Whitmore)

In this report we present some preliminary results from our analysis of $\bar{p}p$ interactions at 14.75 GeV/c. The data are obtained from an 80K picture exposure of the Brookhaven National Laboratory 80-in. bubble chamber. The experimental procedure can be found in two recent preprints submitted to this Conference.[1,2]

This report is divided into four sections :

1) Charged Particle Production

2) Neutral Particle Production

3) Model-Independent Comparisons with High Energy pp Interactions.

4) π^o and Total Particle Multiplicity Distributions.

1. CHARGED PARTICLE PRODUCTION

From measurements of all charged tracks in a sample of $\bar{p}p$ interactions at 14.75 GeV/c, we have determined the inclusive single-particle distributions for the reaction

$$\bar{p}p \to \pi^- + \text{anything}. \qquad (1)$$

At the present time we have not made kinematic fits to inclusive channels. We have, therefore, obtained a sample of $\sim$ 1600 inelastic $\bar{p}p$ interactions (including both annihilation and non-annihilation) by removing elastic 2-prong events by examining missing mass distributions from protons (identified by ionization) and antiprotons (assumed to be any negative particle with a laboratory momentum greater than 9 GeV/c).

Fig. 1 shows the cm rapidity distribution for the reaction (1) where $y = 1/2\ \ell n\ [(E^* + P_L^*)/(E^* - P_L^*)]$. We have made use of the $\bar{p}p$ symmetry by appropriately combining data from reaction (1) with the reaction

$$\bar{p}p \to \pi^+ + \text{anything}. \qquad (2)$$

Also shown in Fig. 1 are data from the reaction

$$pp \to \pi^- + \text{anything} \qquad (3)$$

at 12 and 69 GeV/c[3]. We note that the $\bar{p}p$ data for reaction (1) are more similar in magnitude to the 69 GeV/c data than to the 12 GeV/c data for reaction (3).

A recent paper[4] has studied the energy dependence of the cross section for reaction (1) in the target fragmentation region. This is shown in Fig. 2 along with our measurement at 14.75 GeV/c. We observed that the rapid decrease of this cross section from 9 GeV/c to 14.75 GeV/c is well reproduced by the solid curve which is the result[4] of a multiperipheral model calculation incorporating the strong energy dependence of σ_n (annihilation) and the large annihilation average particle multiplicity.

Fig. 3 shows the rapidity distribution for reaction (1) for the different charge-particle multiplicities. The features are similar to those observed[3] in high energy pp collisions-namely, for low multiplicity the distribution is relatively wide, while for high multiplicity the rapidity distribution is significantly narrower. We are presently attempting to separate reaction (1) into a distribution resulting from annihilation only and one from $\bar{p}p$ non-annihilation interactions.

2. NEUTRAL PARTICLE PRODUCTION

With their characteristic decay or conversion, neutral particles are among the easiest particles to identify in a bubble-chamber experiment. The charged tracks from the decay or conversion can easily be measured and fitted to one of the kinematic hypotheses: $K^o_S \to \pi^+\pi^-$, $\Lambda \to p\pi^-$, $\Lambda \to \pi^+\bar{p}$, and $\gamma(p) \to e^+e^-(p)$. This kind of analysis has been a fruitful part of the bubble-chamber experiments performed at Fermilab, Serpukhov, and other laboratories. Much of our knowledge of the reactions $pp \to \gamma X$, $K^o_S X$, and ΛX is derived from this technique.

In this experiment we have measured a sample of 1107 V^o decays and γ conversions. A detailed analysis is given in Ref. 2. Fig. 4 shows $\sigma_n(V^o)$, the neutral particle cross section, and $\langle V^o \rangle$, the average number of V^o produced per inelastic collision for each charged multiplicity n. The average number of $\langle \pi^o \rangle$ is observed to increase with the associated number of charged particles. This dependence contrasts with results from pp and Kp interactions at comparable energies. This increase in $\langle \pi^o \rangle$ vs n may arise from the fact that there are two processes-annihilation and non-annihilation-in $\bar{p}p$ interactions[5]. This different slope dependence is also observed in $\langle K^o_S \rangle$ vs n. On the other hand Λ production appears similar in pp and $\bar{p}p$ interactions. This suggests that Λ's are produced mainly from target proton fragmentation.

The difference between K_S^o and Λ^o production in $\bar{p}p$ interactions is further studied in Fig. 5 which shows $\sigma(K_S^o)$ and $\sigma(\Lambda)$ as a function of laboratory momentum[2]. While the energy dependence of Λ production in pp and $\bar{p}p$ interactions is similar, this is not true for $\sigma(K_S^o)$ which actually decreases for the $\bar{p}p$ interactions in the momentum range up to 14.75 GeV/c.

Fig. 6 shows the invariant single-particle distributions of γ, K_S^o, and Λ as a function of the Feynman variable $x(= 2p_L^*/\sqrt{s})$. For comparison, data from pp interactions have been interpolated and are represented by solid lines. Note that the average longitudinal momenta for γ and K_S^o are larger in $\bar{p}p$ interactions than in pp interactions. This is indicated by a smaller slope parameter in the x distribution. On the other hand, the Λ distributions are similar in all the reactions considered. The present study of neutral-particle production clearly indicates that there are two production mechanisms in $\bar{p}p$ interactions.

3. MODEL-INDEPENDENT COMPARISONS WITH HIGH ENERGY pp INTERACTIONS

Two questions have often been raised concerning high-energy interactions:

a) As the incident energy increases, how will the inclusive single-particle distributions change?

b) How will the distributions depend on different initial states? There are many plausible answers. One perhaps hopes that a model can be formulated to account for the distributions and their dependencies on energy and initial state. Generally, these models contain many parameters. Another approach in tackling the problem is to set up guidelines, generally in the context of some scaling hypothesis. A well-known example is Feynman scaling which suggests that the invariant single-particle distribution approaches an energy independent form at high energies. That is,

$$E\frac{d^3\sigma}{dp^3} \xrightarrow[s\to\infty]{} f(x, p_T)$$

where $x = 2p_L^*/\sqrt{s}$. Note that the form of $f(x, p_T)$ is not specified.

In this report we consider another hypothesis: in high energy hadron collisions, only the average value in the distribution changes with the incident energy and the initial state. The charged multiplicity distribution is perhaps the best known example. It has been found that while $\langle n_c \rangle$ increases with incident energy, the shape of the charged multiplicity distribution is not strongly

dependent on either the energy or initial state. This was first predicted by Koba, Nielsen, and Olesen[6].

The hypothesis can be expressed more explicitly[7] as follows. Given a distribution $f(x_1, x_2)$ with variables x_1 and x_2, the following scaling equation holds for high energy collisions:

$$f(x_1, x_2) = \frac{1}{\langle x_1 \rangle \langle x_2 \rangle} f\left(\frac{x_1}{\langle x_1 \rangle}, \frac{x_2}{\langle x_2 \rangle}\right) .$$

In the ensuing discussion, we present evidence for this kind of scaling for two cases: (a) charged and neutral multiplicity distributions and (b) distributions in longitudinal (p_L) and transverse momentum (p_T) in the center of mass system.

Fig. 7 shows the distributions in charged multiplicity[1] and associated production[2] of π^o, K^o_S, and Λ in 14.75 GeV/c $\bar{p}p$ interactions. In these distributions, the dependence of the average values has been divided out so they are plotted in the $n_c/\langle n_c \rangle$ variable instead of n_c. The solid curves given in the figure are results of fits to high energy pp data[8]. Except for Λ, the $\bar{p}p$ data lie on the fitted pp curves. The Λ distribution actually looks similar to the low energy pp data and has not yet reached a possible limiting distribution.

Recently we have studied[7] the single particle π^- distribution from pp interactions in the p_T and p_L variables. We found that the distributions from the pp data in the momentum range 13 to 300 GeV/c satisfy the scaling equation. In Fig. 8 we reproduce the single-particle distributions from pp interactions and add our measurement of charged tracks from the $\bar{p}p$ interactions at 14.75 GeV/c in which only the negatively charged tracks in the backward hemisphere and the positively charged tracks in the forward hemisphere are included in the analysis. These tracks are assigned the pion mass. The figure shows that within the present statistics, the proposed hypothesis is satisfied.

It should be emphasized that the scaling hypothesis provides a means of comparing data from different experiments without resorting to specific theoretical models. What remains to be studied is the average value and its dependence on the incident energy and the initial state.

4. π^o AND TOTAL PARTICLE MULTIPLICITY DISTRIBUTIONS

We have made a preliminary study of the π^o and the total particle multiplicity ($n_T = n_c + n_o$) distributions in our experiment. The technique is to scan for

γ conversions in the downstream tantalum plate which is 1/4-in. thick. In the scan we have required: (a) only one beam interaction in every acceptable frame and (b) no indication of shower(s) in the upstream direction. Scanners were also requested to record conversions and to determine whether or not the point to the interaction vertex. The nonpointing conversions provide a background study and constitute less than 10% of the total number of conversions. The end-points of the conversions at the plate were measured. The charged tracks in the chamber were also measured and their ionization was subsequently examined in an effort to identify protons (and antiprotons by reflection in the cm system). The remaining tracks were interpreted as pions. We ran Monte Carlo programs using these charged tracks and assuming that neutral pions behave in the same way kinematically as the charged pions. The Monte Carlo distributions generated from the charged tracks agree well with the measured distributions at the plate.

The average γ conversion probability in this experiment is determined to be 0.44. From a preliminary sample of 2269 γ's, the observed distributions $G(n_\gamma)$ were fitted to give the relative π^o cross sections $H(n_o)$:

$$G(n_\gamma) = \sum_{n_o} H(n_o)\ C(n_\gamma | n_o).$$

where $C(n_\gamma | n_o)$ is the conversion probability of n_γ gammas from n_o pions and is determined from the charged tracks. The values of $H(n_o)$ are normalized to give the π^o cross sections which are shown in Fig. 9. From this sample we determine $\langle n_o \rangle = 1.61 \pm 0.27$ and $f_2^{oo} = \langle n_o(n_o-1) \rangle - \langle n_o \rangle^2 = 0.23 \pm 0.43$.

Fig. 10 shows the total particle multiplicity distributions at our energy. The 10 GeV/c $\pi^+ p$ data obtained from the SLAC 82-in. bubble chamber filled with a Ne-H_2 mixture is also included. It should be noted that n_T in the $\pi^+ p$ distribution has been defined as the number of particles in the final state minus two[9]. The total multiplicity distribution in $\bar{p}p$ interactions shows a rather broad maximum, giving a strong indication that the distribution may indeed consist of two components. Work is under way to separate these components by checking the ionization information of the charged tracks.

REFERENCES

1) F.T. Dao, J. Lach and J. Whitmore, Charged Particle Multiplicity Distributions from 14.75 GeV/c $\bar{p}p$ Interactions, NAL-Pub-73/80-EXP (1974).

2) F.T. Dao, J. Lach and J. Whitmore, Inclusive Neutral Particle Production in 14.75 GeV/c Antiproton Interactions, NAL-Pub-73/81-EXP (1974).

3) See J. Whitmore, Phys. Reports 10C, (1974) 273.

4) S. Humble, CERN preprint TH 1830 - CERN (1974).

5) Private communication from H. Miettinen. Also see paper by T. Kitagaki at this Conference.

6) Z. Koba, H.B. Nielsen and P. Olesen, Nucl. Phys. B40 (1973) 317.

7) F.T. Dao et al., NAL-Pub-74/45-EXP (to be published in Phys. Rev. Letters August 1974).

8) F.T. Dao and J. Whitmore, Phys. Letters 46B (1973) 252 and D. Cohen, Phys. Letters 47B (1973) 457.

9) M.E. Binkley et al., Phys. Letters 45B (1973) 295.

FIGURE CAPTIONS

Fig. 1 Inclusive rapidity distribution for the reaction $\bar{p}p \to \pi^-$ + anything at 14.75 GeV/c.

Fig. 2 Integrated cross sections at $y_{lab} = 0$ for π^- production in pp and $\bar{p}p$ interactions as a function of the incident beam momentum. (From Ref. 4).

Fig. 3 Semi-inclusive rapidity distributions for the reaction $\bar{p}p \to \pi^-$ + (n-1) charged particles + anything at 14.75 GeV/c.

Fig. 4 σ_n and $\langle n_{V^0} \rangle$ as a function of multiplicity for (a) π^0, (b) K^0_S, and (c) Λ. The solid (dotted) line in (a) is a representation of pp data at 12 GeV/c (K^-p data at 14.3 GeV/c).

Fig. 5 Inclusive cross sections for K^0_S and Λ production. The solid curves represent data from pp collisions.

Fig. 6 Invariant cross section and average transverse momentum as a function of x for (a) γ and (b) K^0_S. (c) Invariant cross section for Λ production.

Fig. 7 KNO scaling function for (a) n_c, (b) π^0, (c) K^0_S, and (c) Λ data. The solid curves are obtained from fitting pp data for beam momenta greater than 50 GeV/c (see Ref. 8).

Fig. 8 Single-particle distributions in the scaled variables (a) $p_T/\langle p_T \rangle$ and (b) $p_L/\langle p_L \rangle$ (see Ref. 7).

Fig. 9 π^0 multiplicity distributions for all and associated charged multiplicity. Solid lines are drawn to guide the eye.

Fig. 10 Total particle multiplicity distributions. Solid and dashed lines are drawn to guide the eye. (see Ref. 9 for the π^+p data).

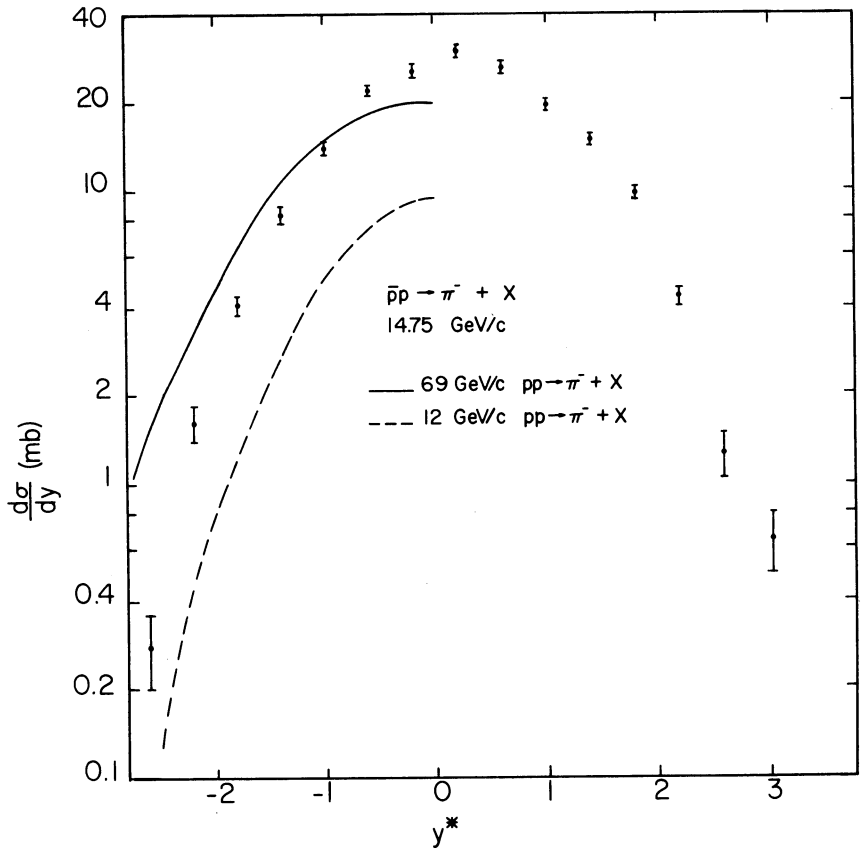
40
20
10
4
2
1
0.4
0.2
0.1
$\frac{d\sigma}{dy}$ (mb)
$\bar{p}p \to \pi^- + X$
14.75 GeV/c
69 GeV/c $pp \to \pi^- + X$
12 GeV/c $pp \to \pi^- + X$
-2
-1
0
1
2
3
y*

Fig. 1

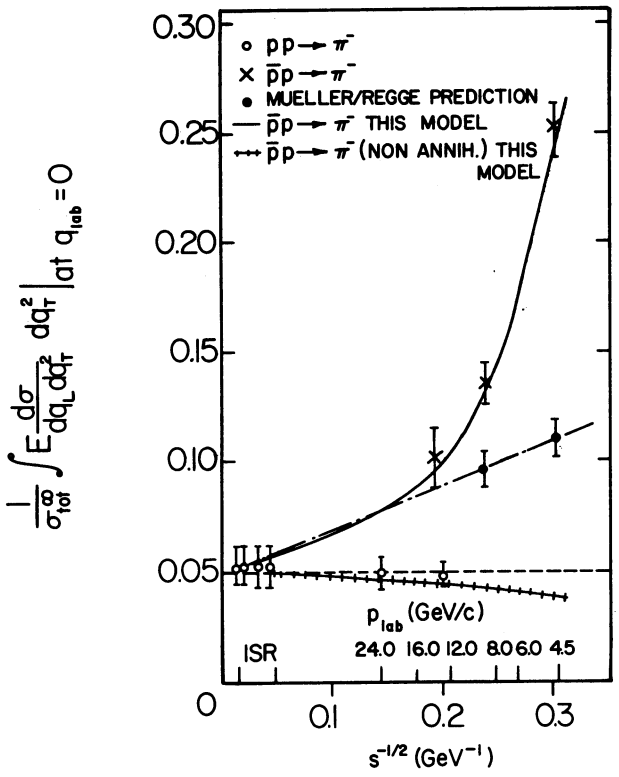
0.30
0.25
0.20
0.15
0.10
0.05
0
$\frac{1}{\sigma_{tot}} \int E \frac{d\sigma}{dq_L dq_T^2} dq_T^2 \Big|_{at\ q_{lab}=0}$
$pp \to \pi^-$
$\bar{p}p \to \pi^-$
MUELLER/REGGE PREDICTION
$\bar{p}p \to \pi^-$ THIS MODEL
$\bar{p}p \to \pi^-$ (NON ANNIH.) THIS MODEL
p_{lab} (GeV/c)
ISR
24.0 16.0 12.0 8.0 6.0 4.5
0.1
0.2
0.3
$s^{-1/2}$ (GeV^{-1})

Fig. 2

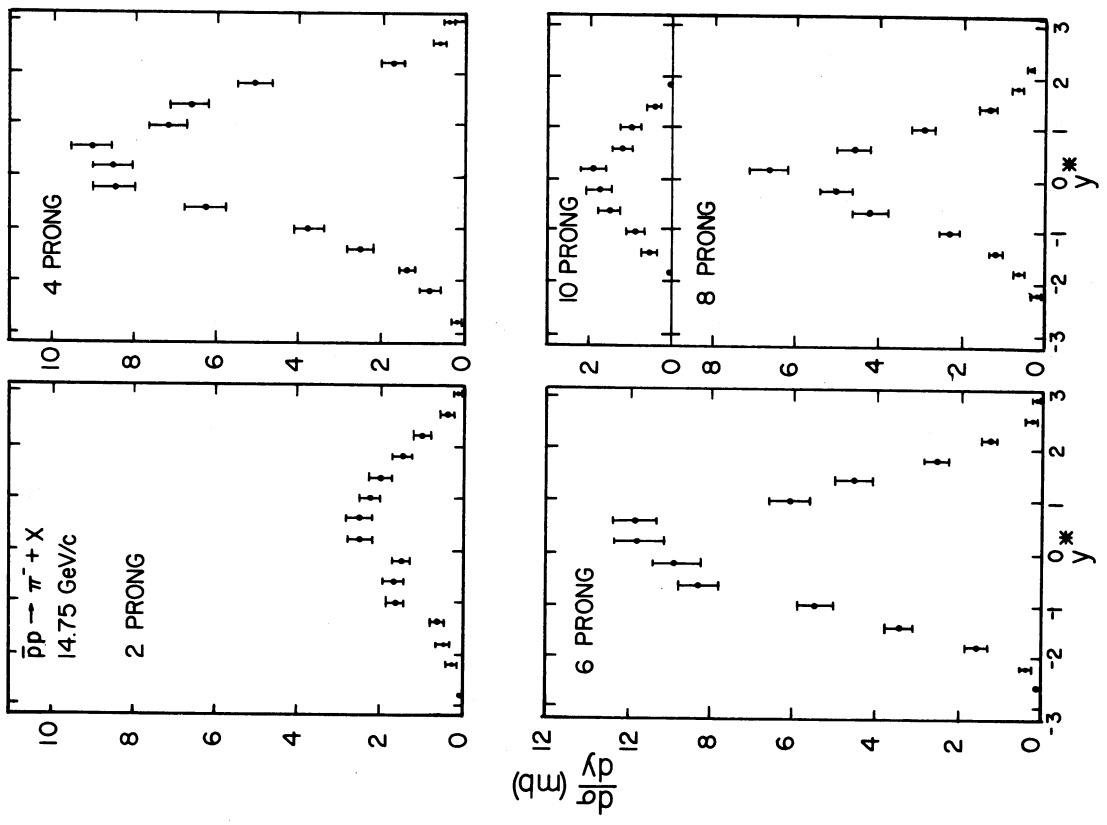
$\bar{p}p \to \pi^- + X$
14.75 GeV/c
2 PRONG
4 PRONG
6 PRONG
8 PRONG
10 PRONG
$\frac{d\sigma}{dy}$ (mb)
y^*

Fig. 3

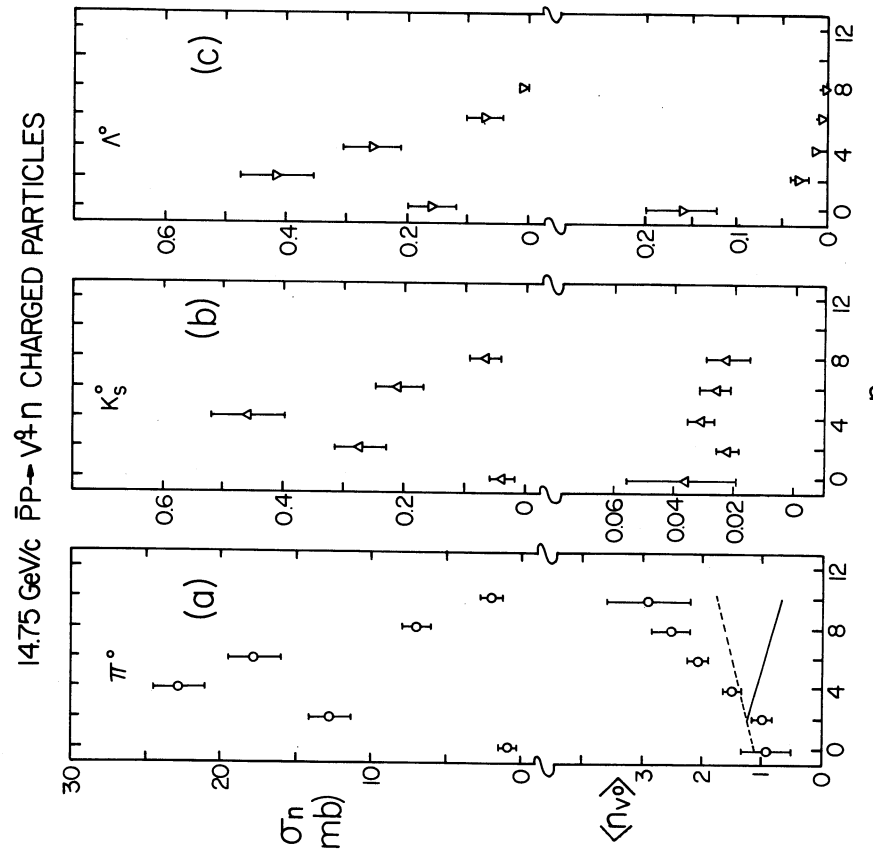
14.75 GeV/c $\bar{P}P \to V^0 + n$ CHARGED PARTICLES
(a)
π^0
(b)
K_S^0
(c)
Λ^0
σ_n (mb)
$\langle n_{V^0} \rangle$
n

Fig. 4

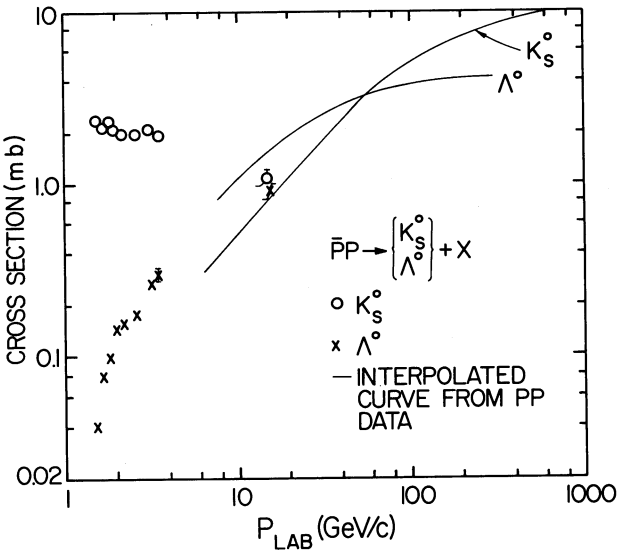
CROSS SECTION (mb)
P_LAB (GeV/c)
K°s
Λ°
P̄P → {K°s, Λ°} + X
K°s
Λ°
INTERPOLATED CURVE FROM PP DATA

Fig. 5

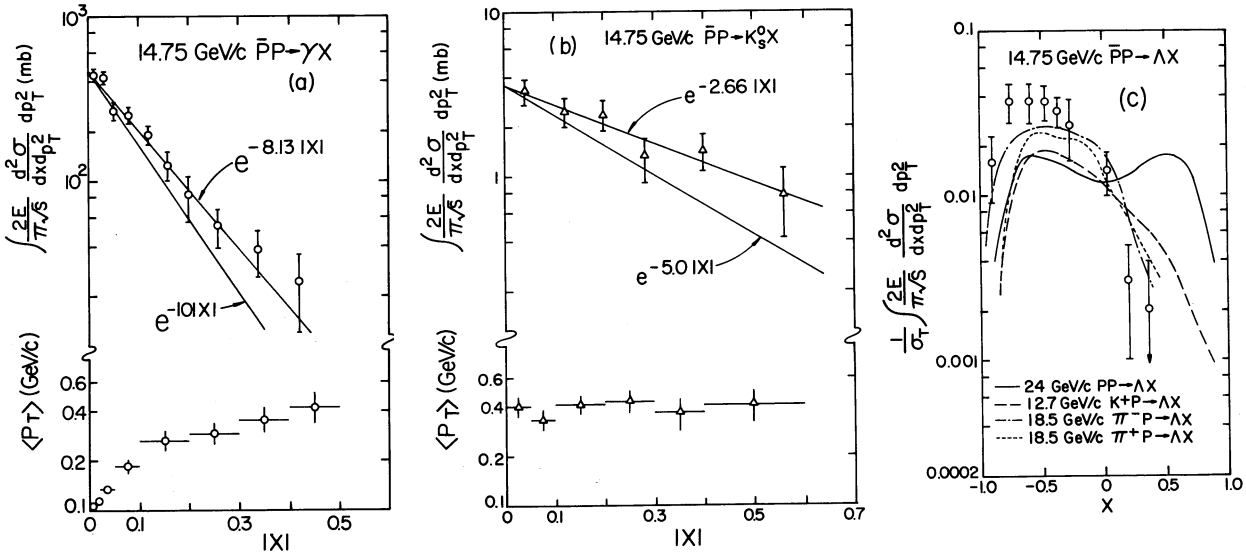
14.75 GeV/c P̄P→γX
(a)
e^-8.13 |X|
e^-10|X|
(b) 14.75 GeV/c P̄P→K°sX
e^-2.66 |X|
e^-5.0 |X|
14.75 GeV/c P̄P→ΛX
(c)
24 GeV/c PP→ΛX
12.7 GeV/c K+P→ΛX
18.5 GeV/c π⁻P→ΛX
18.5 GeV/c π⁺P→ΛX
|X|
X

Fig. 6

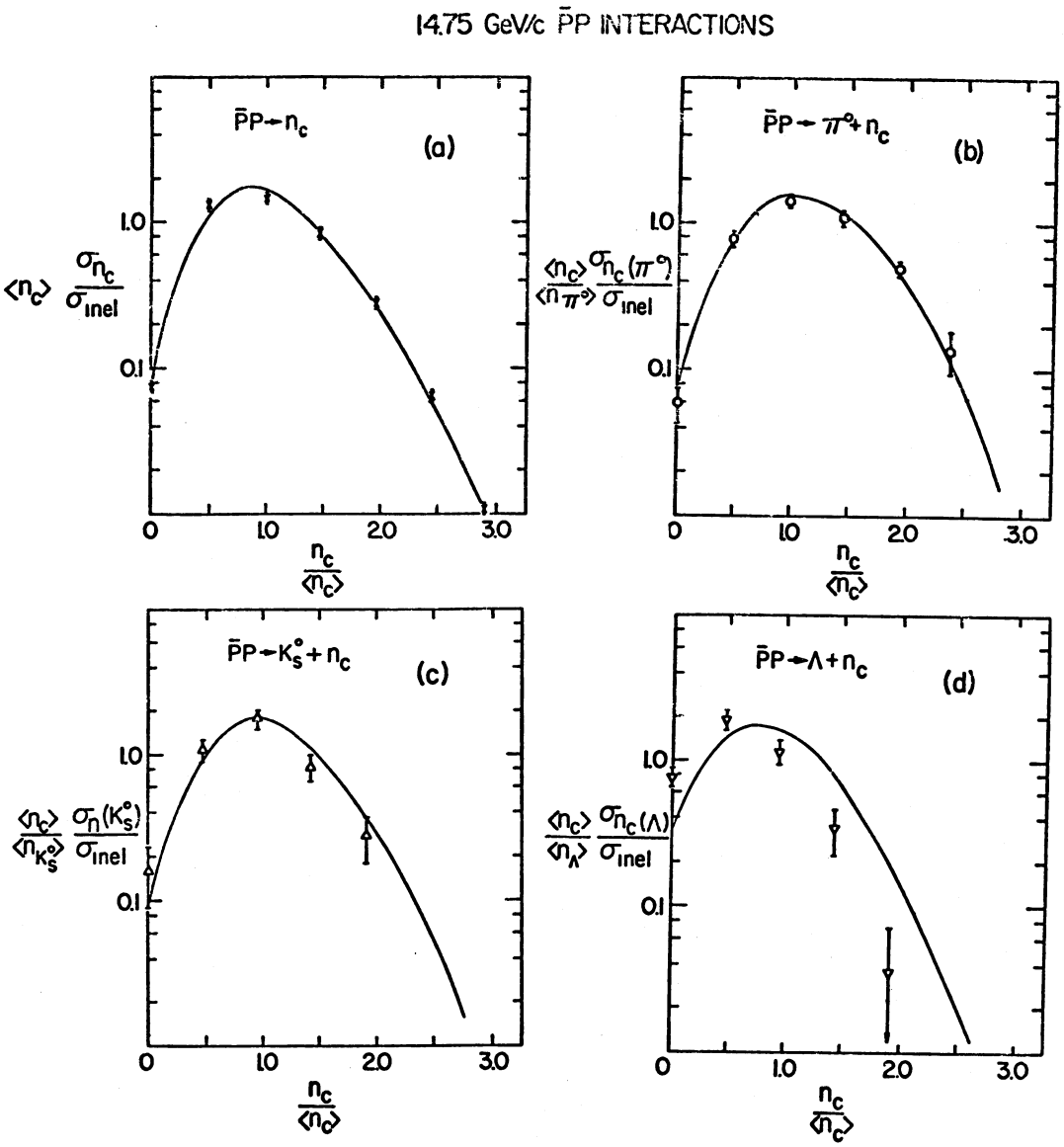
14.75 GeV/c $\bar{P}P$ INTERACTIONS
$\bar{P}P \to n_c$
(a)
$\langle n_c \rangle \frac{\sigma_{n_c}}{\sigma_{inel}}$
$\bar{P}P \to \pi^0 + n_c$
(b)
$\frac{\langle n_c \rangle \sigma_{n_c}(\pi^0)}{\langle n_{\pi^0} \rangle \sigma_{inel}}$
$\bar{P}P \to K_S^0 + n_c$
(c)
$\frac{\langle n_c \rangle}{\langle n_{K_S^0} \rangle} \frac{\sigma_n(K_S^0)}{\sigma_{inel}}$
$\bar{P}P \to \Lambda + n_c$
(d)
$\frac{\langle n_c \rangle}{\langle n_\Lambda \rangle} \frac{\sigma_{n_c}(\Lambda)}{\sigma_{inel}}$
1.0
0.1
0
1.0
2.0
3.0
$\frac{n_c}{\langle n_c \rangle}$

Fig. 7

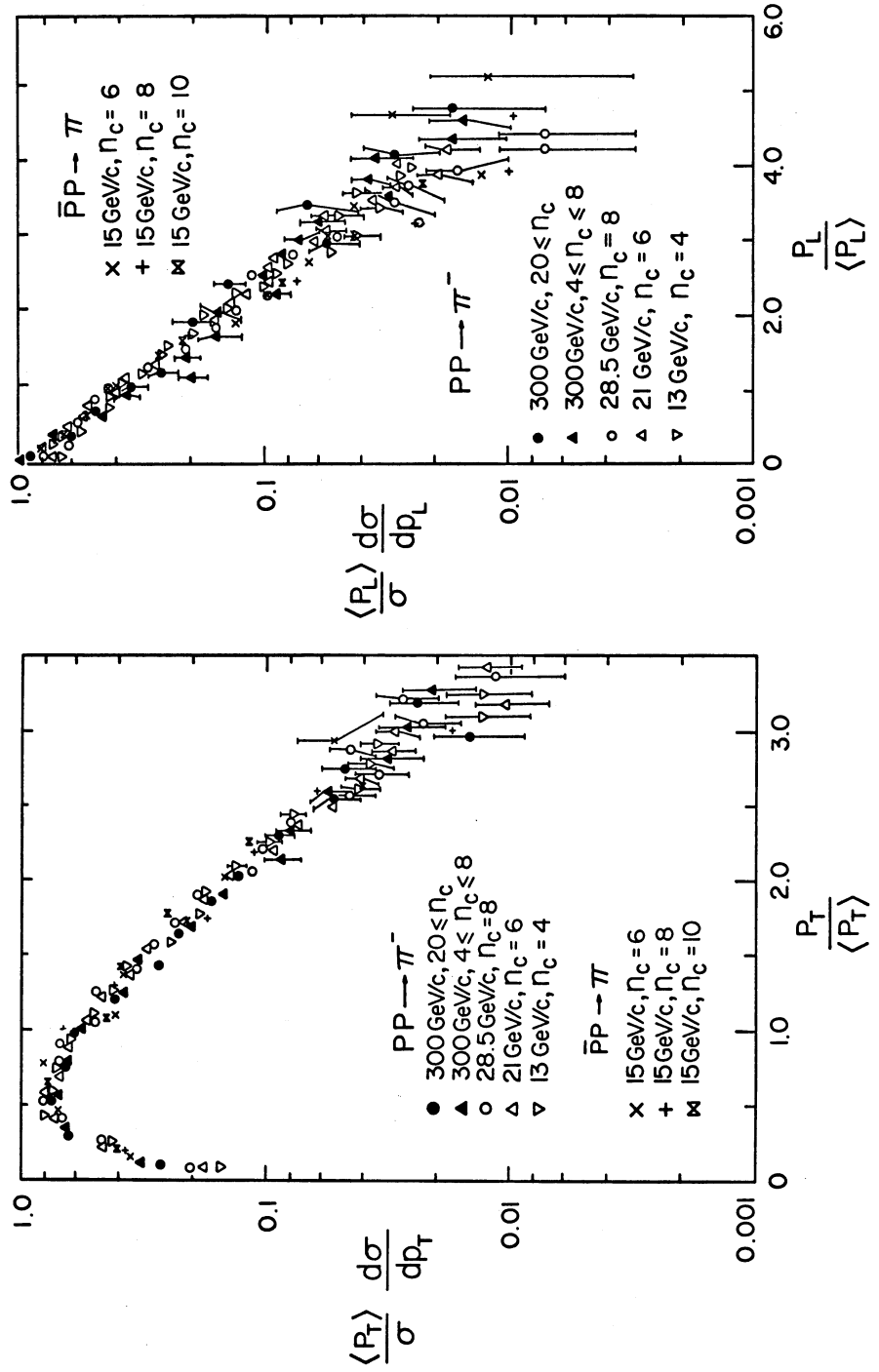
$\bar{P}P \to \pi$
× 15 GeV/c, n_c= 6
+ 15 GeV/c, n_c= 8
⋈ 15 GeV/c, n_c= 10
$PP \to \pi^-$
● 300 GeV/c, 20 ≤ n_c
▲ 300 GeV/c, 4 ≤ n_c ≤ 8
○ 28.5 GeV/c, n_c = 8
△ 21 GeV/c, n_c = 6
▽ 13 GeV/c, n_c = 4
$\frac{\langle P_L \rangle}{\sigma} \frac{d\sigma}{dp_L}$
$\frac{P_L}{\langle P_L \rangle}$
1.0
0.1
0.01
0.001
0
2.0
4.0
6.0
$PP \to \pi^-$
● 300 GeV/c, 20 ≤ n_c
▲ 300 GeV/c, 4 ≤ n_c ≤ 8
○ 28.5 GeV/c, n_c = 8
△ 21 GeV/c, n_c = 6
▽ 13 GeV/c, n_c = 4
$\bar{P}P \to \pi$
× 15 GeV/c, n_c = 6
+ 15 GeV/c, n_c = 8
⋈ 15 GeV/c, n_c = 10
$\frac{\langle P_T \rangle}{\sigma} \frac{d\sigma}{dp_T}$
$\frac{P_T}{\langle P_T \rangle}$
1.0
0.1
0.01
0.001
0
1.0
2.0
3.0

Fig. 8

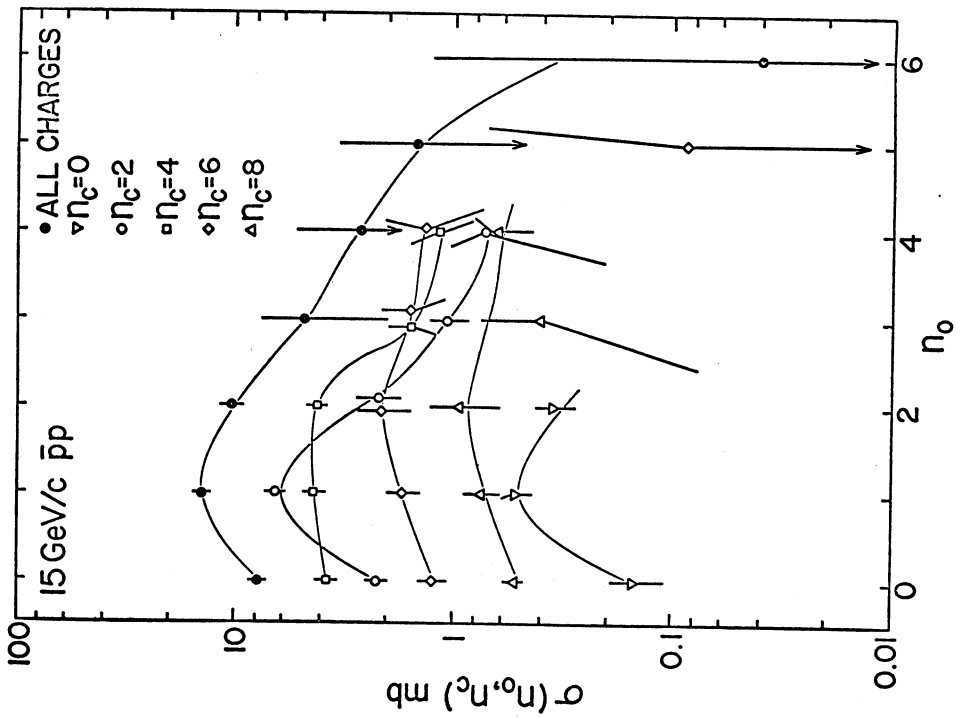
15 GeV/c p̄p
• ALL CHARGES
▽ n_c=0
○ n_c=2
□ n_c=4
◇ n_c=6
△ n_c=8
σ (n_o,n_c) mb
n_o
100
10
1
0.1
0.01
0
2
4
6

Fig. 9

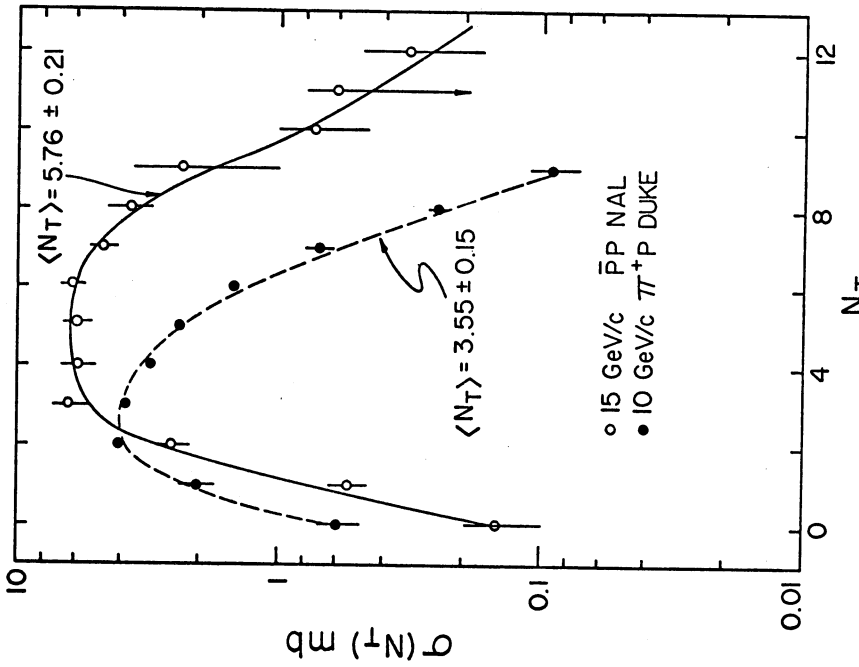
⟨N_T⟩= 5.76 ± 0.21
⟨N_T⟩= 3.55 ± 0.15
○ 15 GeV/c p̄p NAL
● 10 GeV/c π⁺p DUKE
σ (N_T) mb
N_T
10
1
0.1
0.01
0
4
8
12

Fig. 10

D I S C U S S I O N

- *Smith:*

Did you compare your scaling function in transverse momenta to the ISR data at high transverse momenta?

- *Dao:*

No, I did not, because the scaling function is controlled by $\langle p_T \rangle$, which is difficult to obtain from ISR data.

- *Šimák:*

Do you see any difference between transverse momenta of kaons and pions?

- *Dao:*

At 15 GeV/c I have not yet seen these distributions.

- *Malhotra:*

Did you try to see any scaling in the total momentum $p/\langle p \rangle$?

- *Dao:*

We did not try it, but it seems to me that different variables are not as important as the general concept of this scaling. Some of my colleagues try to use the rapidity, which is interesting from the point of view of the existence of a plateau.